

# Re-investigation of the crystal structure of whewellite $[\text{Ca}(\text{C}_2\text{O}_4)\cdot\text{H}_2\text{O}]$ and the dehydration mechanism of caoxite $[\text{Ca}(\text{C}_2\text{O}_4)\cdot 3\text{H}_2\text{O}]$

T. ECHIGO<sup>1,\*</sup>, M. KIMATA<sup>1</sup>, A. KYONO<sup>1</sup>, M. SHIMIZU<sup>1</sup> AND T. HATTA<sup>2</sup>

<sup>1</sup> Earth Evolution Sciences, Graduate School of Life and Environmental Sciences, University of Tsukuba, Tennoudai 1-1-1, Tsukuba 305-8572, Japan

<sup>2</sup> Japan International Research Center for Agricultural Sciences, Independent Administrative Institute, Ohwashi 1-1, Tsukuba 305-8686, Japan

## ABSTRACT

The crystal structure of whewellite  $[\text{Ca}(\text{C}_2\text{O}_4)\cdot\text{H}_2\text{O}]$  and the dehydration mechanism of caoxite  $[\text{Ca}(\text{C}_2\text{O}_4)\cdot 3\text{H}_2\text{O}]$  have been studied by means of differential thermal analysis, X-ray diffraction (powder and single-crystal) analysis and infrared analysis. The first and second analyses confirmed the direct transformation of caoxite into whewellite without an intermediate weddellite  $[\text{Ca}(\text{C}_2\text{O}_4)\cdot 2\text{H}_2\text{O}]$  stage. Infrared spectra obtained from caoxite, weddellite and whewellite emphasize the similarity of the O–H-stretching band and O–C–O-stretching band in whewellite and caoxite and the unique bands of weddellite. The structure refinement at low temperature (123 K) reveals that all the hydrogen atoms of whewellite form hydrogen bonds and the two water molecules prop up the crystal structure by the hydrogen bonds that cause a strong anisotropy of the displacement parameter.

Comparing the structural features of whewellite with those of weddellite and caoxite suggests that caoxite and whewellite have a sheet structure consisting of  $\text{Ca}^{2+}$  ions and oxalate ions although weddellite does not. It is additionally confirmed that the sheets of caoxite are corrugated by hydrogen bonds but whewellite has flat sheets. The corrugated sheets of caoxite would be flattened by dehydration so the direct transformation of caoxite into whewellite would not occur via weddellite. Essential for this transformation is the dehydration of interlayered water molecules in caoxite leading to the building of the crystal structure of whewellite on its intralayered water molecules. The difference in conformation of water molecules between those two crystal structures may explain the more common occurrence of whewellite than of caoxite in nature.

**KEYWORDS:** whewellite, caoxite, weddellite, dehydration mechanism, crystal structure, X-ray diffraction, infrared analysis, differential thermal analysis.

## Introduction

WHEWELLITE  $[\text{Ca}(\text{C}_2\text{O}_4)\cdot\text{H}_2\text{O}]$  is a calcium oxalate monohydrate mineral found naturally in plant tissues, in sediments (as a mineral of organic origin) and in urinary stones (Gaines *et al.*, 1997). Weddellite  $[\text{Ca}(\text{C}_2\text{O}_4)\cdot 2\text{H}_2\text{O}]$  and caoxite  $[\text{Ca}(\text{C}_2\text{O}_4)\cdot 3\text{H}_2\text{O}]$  have also been generally

accepted to represent calcium oxalate hydrate minerals (Gaines *et al.*, 1997; Basso *et al.*, 1997). These crystal structures are characterized by edge-shared  $\text{CaO}_8$  polyhedra that constitute the linkage between oxalate ions  $[(\text{C}_2\text{O}_4)^{2-}]$  (Basso *et al.*, 1997). On the basis of the polyhedron model, caoxite, weddellite and whewellite are composed of dimers, chains and sheets, respectively (Basso *et al.*, 1997). There has been growing speculation and some evidence that caoxite could be a precursor in weddellite and whewellite formation (Tomazic and Nancollas, 1979). However, the

\* E-mail: echigo@arsia.geo.tsukuba.ac.jp  
DOI: 10.1180/0026461056910235

actual dehydration process of synthetic coaxite was characterized by the direct transformation into whewellite at 116.5°C without an intermediate weddellite stage (Morishige *et al.*, 1999). Hence, speculation about transformation of coaxite into weddellite is inconsistent with the experimental result.

Many structure analyses of calcium oxalate hydrate minerals have been reported (whewellite: Hoffman, 1961, Cocco, 1961; Cocco and Sabelli, 1962; Arnott *et al.*, 1965; Leavens, 1968; Tazzoli and Domeneghetti, 1980; Deganello and Piro, 1981; weddellite: Stering, 1965; Tazzoli and Domeneghetti, 1980; and coaxite: Deganello *et al.*, 1981; Basso *et al.*, 1997). Though all hydrogen atoms of the water molecules of both weddellite and coaxite were reasonably located, the positions of one in four hydrogen atoms in whewellite were not established (Tazzoli and

Domeneghetti, 1980). Considering the conformation of the water molecules, it may be topologically impossible for mere condensation of  $\text{CaO}_8$  polyhedra to explain the transformation of one structure into the next (Deganello *et al.*, 1981). Thus, it is necessary to determine the hydrogen atom position in order to understand the dehydration mechanism of those three minerals. X-ray data collection at low temperature may reduce thermal vibration of the water molecules and lead to accurate determination of the hydrogen position. Furthermore, IR spectra of the calcium oxalate minerals could provide useful information for understanding the geometry and orientation of the cation ( $\text{Ca}^{2+}$ )–anion  $[(\text{C}_2\text{O}_4)^{2-}]$  bonds as well as hydrogen bonds.

The purpose of this paper is to refine the crystal structure of whewellite at low temperature (123 K), to interpret the role of water

TABLE 1. Summarized crystal data and details of refinement parameters.

Chemical formula	$\text{Ca}(\text{C}_2\text{O}_4)\cdot\text{H}_2\text{O}$
Formula weight	146.11
Crystal dimensions	0.50 x 0.40 x 0.30 mm
Diffractometer	Rigaku RAXIS-RAPID
Radiation	Mo- $K\alpha$ ( $\lambda = 0.71069 \text{ \AA}$ )
Monochromator	graphite
Voltage, current	50 kV, 40 mA
$2\theta_{\text{max}}$	55°
Structure refinement	Full-matrix least-squares on $F^2$
Temperature	123(1) K
Lattice parameters	
$a$	6.250(1) $\text{\AA}$
$b$	14.471(2) $\text{\AA}$
$c$	10.114(2) $\text{\AA}$
$\beta$	109.978(5)°
$V$	859.7(3) $\text{\AA}^3$
$Z$	8
$D_{\text{calc}}$	2.258 $\text{g/cm}^3$
Space group	$P2_1/c$ (#14)
F000	592
$\mu(\text{Mo-}K\alpha)$	13.68 $\text{cm}^{-1}$
Measured reflections	5454
Independent refractions, $R_{\text{int}}$	1908, 0.050
$R1$ , $wR2$ (all data)	0.054, 0.091
Observed refractions [ $I_o > 2\sigma(I_o)$ ]	1688
Parameters used in the refinement	161
Reflection/parameter ratio	10.48
$R1$ [ $I_o > 2\sigma(I_o)$ ]	0.041
$wR2$ [ $I_o > 2\sigma(I_o)$ ]	0.038
Goodness of fit indicator	1.12
Max. peak in final diff. map	0.77 $\text{e/\AA}^3$
Min. peak in final diff. map	-1.51 $\text{e/\AA}^3$

molecules in the crystal structure, and to understand the mechanism of the dehydration of caoxite.

## Experimental method

Samples of whewellite and weddellite were selected from specimens from Bilina, in the Czech Republic and from human urinary calculus, respectively. The samples and their purity were verified by X-ray diffraction (XRD) (powder and single-crystal) analysis. Caosite was synthesized according to the method suggested by Morishige *et al.* (1999): dimethyl oxalate ( $C_4H_6O_4$ ) and anhydrous calcium chloride ( $CaCl_2$ ) were used as starting compounds. The caosite crystals were synthesized at room temperature (23°C) by reaction of aqueous solution of dimethyl oxalate with an aqueous solution of anhydrous calcium chloride in a stoichiometric proportion. The reaction was induced in a glass cup for 72 h and the products deposited in the bottom of the cup were colourless single crystals up to 1 mm long with optical quality. The precipitates were washed with distilled water, filtered and dried. They were found to consist of caosite alone by powder XRD analysis.

Thermal analysis of synthetic caosite was carried out with a thermogravimetric analyser (Rigaku Thermo plus TG8120) in air to attempt to unravel the process of dehydration and identify the dehydrated phase. Approximately 15 mg of the pulverized caosite were heated in an open platinum crucible at the rate of 2.0°C/min up to 1000°C, then four weight-loss steps were confirmed (85.1, 166.9, 424.7 and 724.9°C). Subsequently, the same amount of the powdered

caosite as in the initial sample was heated up to 120, 280, 550 and 1000°C under the same condition as the initial one, then each product was identified by powder XRD.

A single crystal of whewellite was chosen for XRD at 123 K measured with an imaging-plate diffractometer system (Rigaku RAXIS-RAPID, Mo- $K\alpha$  radiation, graphite monochromator) connected to a liquid nitrogen cryostat (Enraf-Nonius FR558NH). The sample was carefully immersed in liquid nitrogen for 6 days, and it was taken out and remounted immediately onto the diffractometer maintained at 123 K. After cooling at 123 K for 1 h, data collection was performed (Table 1). Intensity data were corrected for Lorentz, absorption and polarization effects.

Starting positional parameters were taken from Tazzoli and Domeneghetti (1980) and the unknown position of H(12) was determined on a three-dimensional difference-Fourier map (DIRDIF-99: Beurskens *et al.*, 1999). Structure refinement was carried out using full-matrix least-squares analyses on  $F^2$  (CRYSTALS: Watkin *et al.*, 1996) with anisotropic displacement parameters for non-hydrogen atoms and isotropic ones for hydrogen atoms. The locations of hydrogen positions were determined around the associated oxygen under the restrictions on O–H bond distances (0.96±0.01 Å) and H–O–H angles (104.5±0.5°).

The Fourier transform infrared (FTIR) studies were carried out using a Janssen-type micro-FTIR spectrometer (JASCO corp.) which is capable of working in the region from 4600 to 650  $cm^{-1}$ . Single crystals of whewellite, weddellite and caosite ~20  $\mu m$  thick were chosen under a stereomicroscope and placed on a KBr plate.

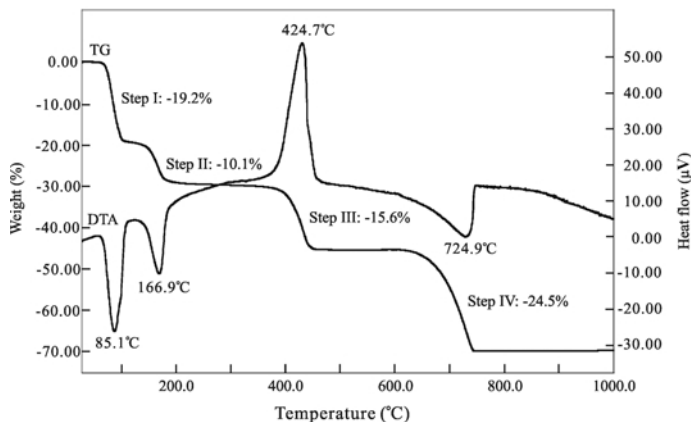


FIG. 1. Thermogravimetric analysis of synthetic caosite.

TABLE 2. Atomic coordinates and displacement parameters ( $\text{\AA}^2$ ) for whewellite at 123 K.

Atom	$x$	$y$	$z$	$B_{\text{eq}}$	$U_{11}$	$U_{22}$	$U_{33}$	$U_{12}$	$U_{13}$	$U_{23}$
C(1)	0.9770(2)	0.32008(9)	0.2439(1)	0.49(2)	0.0039(6)	0.0075(7)	0.0072(6)	0.0005(5)	0.0021(5)	0.0010(5)
C(2)	0.9983(2)	0.42690(9)	0.2505(1)	0.51(2)	0.0048(6)	0.0073(7)	0.0074(6)	0.0011(5)	0.0021(5)	-0.0000(5)
C(3)	0.5147(2)	0.12697(9)	0.1804(1)	0.53(2)	0.0083(6)	0.0037(6)	0.0086(6)	0.0005(5)	0.0034(5)	0.0010(5)
C(4)	0.4426(2)	0.11592(9)	0.3132(1)	0.62(2)	0.0073(6)	0.0078(6)	0.0096(6)	0.0013(5)	0.0042(5)	0.0001(5)
O(1)	0.9665(2)	0.28174(7)	0.1303(1)	0.65(2)	0.0102(5)	0.0086(5)	0.0061(4)	0.0014(4)	0.0033(4)	0.0012(4)
O(2)	0.9898(2)	0.46552(7)	0.1375(1)	0.66(2)	0.0107(5)	0.0092(5)	0.0056(4)	-0.0005(4)	0.0035(4)	-0.0005(4)
O(3)	0.9707(2)	0.28100(7)	0.3537(1)	0.65(2)	0.0105(5)	0.0084(5)	0.0058(4)	0.0004(4)	0.0028(4)	-0.0004(4)
O(4)	0.9898(2)	0.46559(7)	0.3600(1)	0.61(2)	0.0101(5)	0.0078(5)	0.0057(4)	0.0005(4)	0.0034(4)	0.0004(4)
O(5)	0.3573(2)	0.14503(8)	0.0684(1)	0.86(2)	0.0063(4)	0.0186(5)	0.0073(5)	-0.0019(4)	0.0016(4)	-0.0022(4)
O(6)	0.7378(2)	0.12132(7)	0.2051(1)	0.61(2)	0.0056(4)	0.0116(5)	0.0059(4)	0.0001(4)	0.0019(4)	-0.0002(4)
O(7)	0.2793(2)	0.12102(7)	0.3031(1)	0.56(2)	0.0053(4)	0.0100(5)	0.0062(4)	0.0001(4)	0.0022(4)	0.0001(4)
O(8)	0.6025(2)	0.10490(8)	0.4269(1)	0.90(2)	0.0065(4)	0.0206(6)	0.0069(4)	-0.0004(4)	0.0020(4)	-0.0014(4)
Ca(1)	0.96197(4)	0.12372(2)	0.05344(3)	0.393(5)	0.0049(1)	0.0063(1)	0.0038(1)	-0.00007(9)	0.00163(9)	-0.00003(9)
Ca(2)	0.99212(4)	0.12283(2)	0.43515(3)	0.384(5)	0.0048(1)	0.0061(1)	0.0038(1)	-0.00014(9)	0.00157(9)	-0.00004(9)
W(1)	0.3873(2)	0.34435(8)	0.1009(1)	0.92(2)	0.0096(5)	0.0163(6)	0.0094(5)	0.0008(4)	0.0037(4)	0.0027(4)
W(2)	0.5850(2)	0.3926(1)	0.3890(1)	1.74(2)	0.0076(5)	0.0491(8)	0.0082(5)	-0.0011(5)	0.0012(4)	-0.0010(5)
H(11)	0.479(4)	0.367(1)	0.049(2)	3.5(6)						
H(12)	0.388(3)	0.2792(7)	0.091(2)	1.5(4)						
H(21)	0.473(3)	0.378(2)	0.431(2)	6.6(9)						
H(22)	0.513(3)	0.378(2)	0.291(1)	3.6(6)						

Each spectrum was measured in the region of 4000 to 650  $\text{cm}^{-1}$ , with 1  $\text{cm}^{-1}$  resolution and 1000 scans were taken at room temperature.

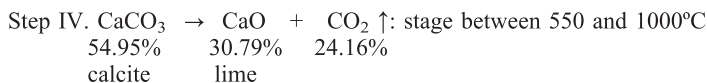
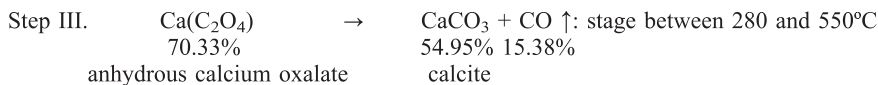
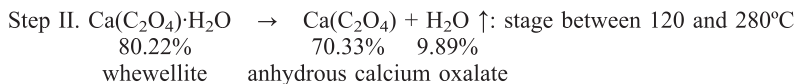
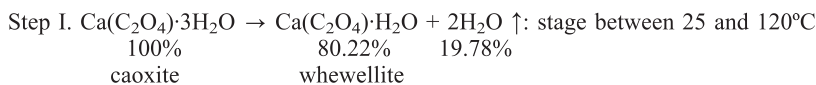
## Results and discussion

Thermogravimetry of synthetic caoxite up to 1000°C is shown in Fig. 1. Four weight loss steps observed at 85.1, 166.9, 424.7 and 724.9°C are 19.2%, 10.1%, 15.6% and 24.5% respectively, though Morishige *et al.* (1999) reported these steps at 116.5, 178.1, 471.4 and 729.0°C. Such differences between these two thermal analyses may be attributed to the conditions under which

the experiments were performed: heating rate, sample weight, and the nature and flow rate of the sweeping gas (Simons and Newkirk, 1964). The product at each weight-loss step was identified as whewellite [ $\text{Ca}(\text{C}_2\text{O}_4)\cdot\text{H}_2\text{O}$ ] at 25 to 120°C, whewellite [ $\text{Ca}(\text{C}_2\text{O}_4)\cdot\text{H}_2\text{O}$ ] at 120 to 280°C, calcite [ $\text{CaCO}_3$ ] at 280 to 550°C and lime [ $\text{CaO}$ ] at >550°C, respectively, by powder XRD analysis.

On the basis of the present thermal decomposition of caoxite (Fig. 1), the explanation has been proposed that four weight loss steps are involved (see below):

Except for  $\text{Ca}(\text{C}_2\text{O}_4)$  of Step II, the products of the proposed process were the same as those in



WHEWELLITE AND CAOXITE

TABLE 3. Bond lengths (Å) and angles (°).

Oxalate group		Calcium polyhedra	
C(1)–C(2)	1.553(2)	Ca(1)–O(1)	2.412(1)
C(3)–C(4)	1.555(2)	Ca(1)–O(3) <sup>a</sup>	2.462(1)
Mean	1.554	Ca(1)–O(4) <sup>b</sup>	2.428(1)
		Ca(1)–O(4) <sup>a</sup>	2.426(1)
C(1)–O(1)	1.257(2)	Ca(1)–O(5) <sup>c</sup>	2.443(1)
C(1)–O(3)	1.259(2)	Ca(1)–O(6)	2.424(1)
C(2)–O(2)	1.258(2)	Ca(1)–O(7) <sup>c</sup>	2.461(1)
C(2)–O(4)	1.258(2)	Ca(1)–W(2) <sup>a</sup>	2.386(1)
C(3)–O(5)	1.248(2)	Mean	2.430
C(3)–O(6)	1.243(2)		
C(4)–O(7)	1.248(2)	Ca(2)–O(1) <sup>d</sup>	2.458(1)
C(4)–O(8)	1.242(2)	Ca(2)–O(2) <sup>b</sup>	2.397(1)
Mean	1.252	Ca(2)–O(2) <sup>d</sup>	2.404(1)
		Ca(2)–O(3)	2.421(1)
O(1)–C(1)–O(3)	126.9(1)	Ca(2)–O(6)	2.427(1)
O(2)–C(2)–O(4)	127.0(1)	Ca(2)–O(7) <sup>c</sup>	2.421(1)
O(5)–C(3)–O(6)	126.6(1)	Ca(2)–O(8)	2.422(1)
O(7)–C(4)–O(8)	126.8(1)	Ca(2)–W(1) <sup>e</sup>	2.512(1)
Mean	126.8	Mean	2.433
O(3)–C(1)–C(2)	116.61(12)		
O(1)–C(1)–C(2)	116.50(12)		
O(2)–C(2)–C(1)	116.63(12)		
O(4)–C(2)–C(1)	116.41(12)		
O(6)–C(3)–C(4)	117.3(1)		
O(5)–C(3)–C(4)	116.1(1)		
O(7)–C(4)–C(3)	116.6(1)		
O(8)–C(4)–C(3)	116.6(1)		
Mean	116.6		

Notes: Symmetry codes: (a)  $x, -y+1/2, z-1/2$  (b)  $-x+2, y-1/2, -z+1/2$  (c)  $x+1, y, z$  (d)  $x, -y+1/2, z+1/2$  (e)  $x+1, -y+1/2, z+1/2$

the present experiments. The real product of Step II was identified as whewellite produced from the rapid absorption of water at room temperature. This result suggests that anhydrous calcium oxalate is prevented from occurring naturally by the strong absorption of water. In addition, it is

evident from the present experiment that caoxite transforms into whewellite, not via weddellite, but by dehydration (Step I). This observation is in accordance with the mechanism proposed by Morishige *et al.* (1999). The present process of pyrolysis of whewellite that corresponds with

TABLE 4. Hydrogen bonds.

	D–H (Å)	H···A (Å)	D···A (Å)	D–H···A (°)
$W(1)–H(11)···O(8)^a$	0.95(3)	1.7(1)	2.902(2)	167.8(1)
$W(1)–H(12)···O(5)$	0.948(9)	2.0(2)	2.658(1)	174.1(1)
$W(2)–H(21)···O(5)^b$	0.96(2)	1.81(5)	2.836(2)	158.0(2)
$W(2)–H(22)···W(1)$	0.96(1)	1.9(2)	2.716(2)	176.1(1)
Mean	0.95	1.85	2.778	169.0

Notes: Symmetry codes: (a)  $x, -y+1/2, z-1/2$  (b)  $x, -y+1/2, z+1/2$

Steps II to IV matches with those previously reported (Frost and Weier, 2003, 2004; Kloprogge *et al.*, 2004).

According to the present structure refinement, the final discrepancy index was  $R = 0.041$  for the 1675 observed reflections at 123 K (Table 1). Atomic positional parameters and anisotropic displacement factors are given in Table 2. The  $x$  coordinates of H(21) and H(22) refined from the low-temperature data are slightly different from those reported by Tazzoli and Domeneghetti (1980). This difference resulted from the measurement at 123 K and our restriction on O–H-bond distances ( $0.96 \pm 0.01$  Å) and H–O–H angles ( $104.5 \pm 0.5^\circ$ ). Selected bond distances and angles are summarized in Table 3 and the geometry of hydrogen bonds is listed in Table 4. The crystal structure of whewellite at 123 K coincides with that at room temperature reported by Tazzoli and Domeneghetti (1980) except for H(12). The present structure analysis at low temperature reveals that all four hydrogen atoms of the water molecules form hydrogen bonds in the crystal structure (Table 4). Additionally, the splitting-oxygen model proposed by Tazzoli and Domeneghetti (1980) is found to be unrealistic for the structural interpretation. The present determination that each water molecule completely occupies the distinctive atom position is reasonable for the next thermal vibration analysis.

The larger displacement parameter of  $W(2)$  suggests the anomalous vibration behavior, and  $W(1)$  also has a large thermal displacement parameter as compared with other oxygen atoms (Table 2). Considering the environmental arrangement of  $W(1)$  and  $W(2)$ ,  $W(1)$  is located near the centre of the tetrahedron formed by Ca(2), O(5), O(8) and  $W(2)$ , including three hydrogen bonds: H(11)⋯O(8), H(12)⋯O(5) and H(22)⋯ $W(1)$  (Fig. 2a). On the other hand,  $W(2)$  is located near the centre of the triangular plane formed by Ca(1), O(5) and  $W(1)$ , containing two hydrogen bonds: H(21)⋯O(5) and H(22)⋯ $W(1)$  (Fig. 2b). The two-dimensional bonds forming the triangular plane impose restraints on the thermal vibration of  $W(2)$ , and the three-dimensional bonds forming the tetrahedron above do likewise for  $W(1)$ . Consequently, it is reasonable to assume that  $W(2)$  can easily vibrate perpendicular to the triangular plane. This is verified by the observation that  $U_{22}$  of  $W(2)$  is especially large among the anisotropic thermal parameters (Table 2).

In whewellite, oxalate groups alternate with the  $\text{Ca}^{2+}$  ions, and both form chains lying in the (010)

plane and running along  $a$  (Fig. 3a). Viewing along  $a$ , adjacent chains are bound together by independent oxalate ions lying in the (100) plane to form the structure with chain-oxalate sheets (Fig. 3b). In the (010) plane, the two intralayered water molecules, H(11)– $W(1)$ –H(12) and H(21)– $W(2)$ –H(22), are arranged along  $c$ . Consequently, the hydrogen bond through H(22) between the two intralayered water molecules exists (Tazzoli and Domeneghetti, 1980) and contributes meaningfully to the construction of the sheet structure (Fig. 3a). Crystal structures of caoxite (Deganello *et al.*, 1980) and weddellite (Tazzoli and

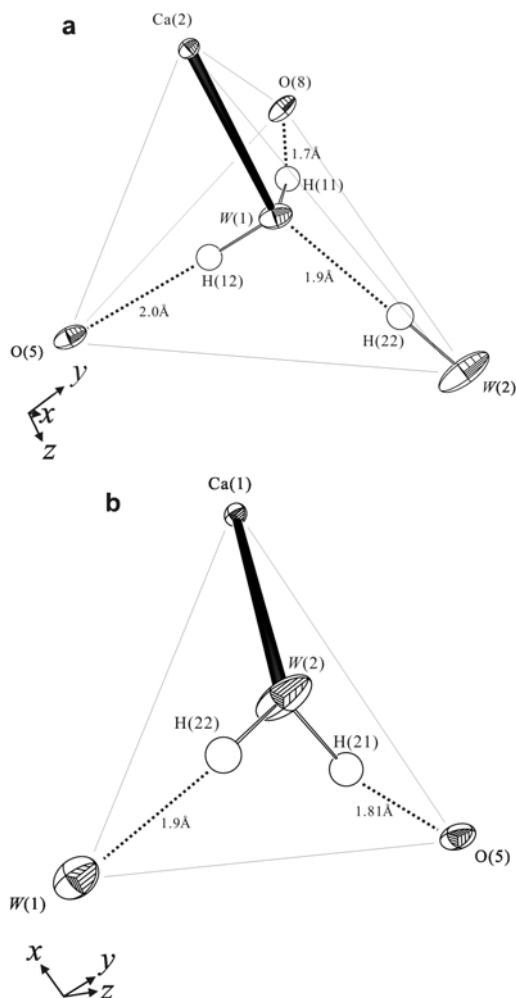


FIG. 2. (a) ORTEP representations of the area around the (a)  $W(1)$  site of whewellite at 123 K, and (b) the  $W(2)$  site of whewellite at 123 K.

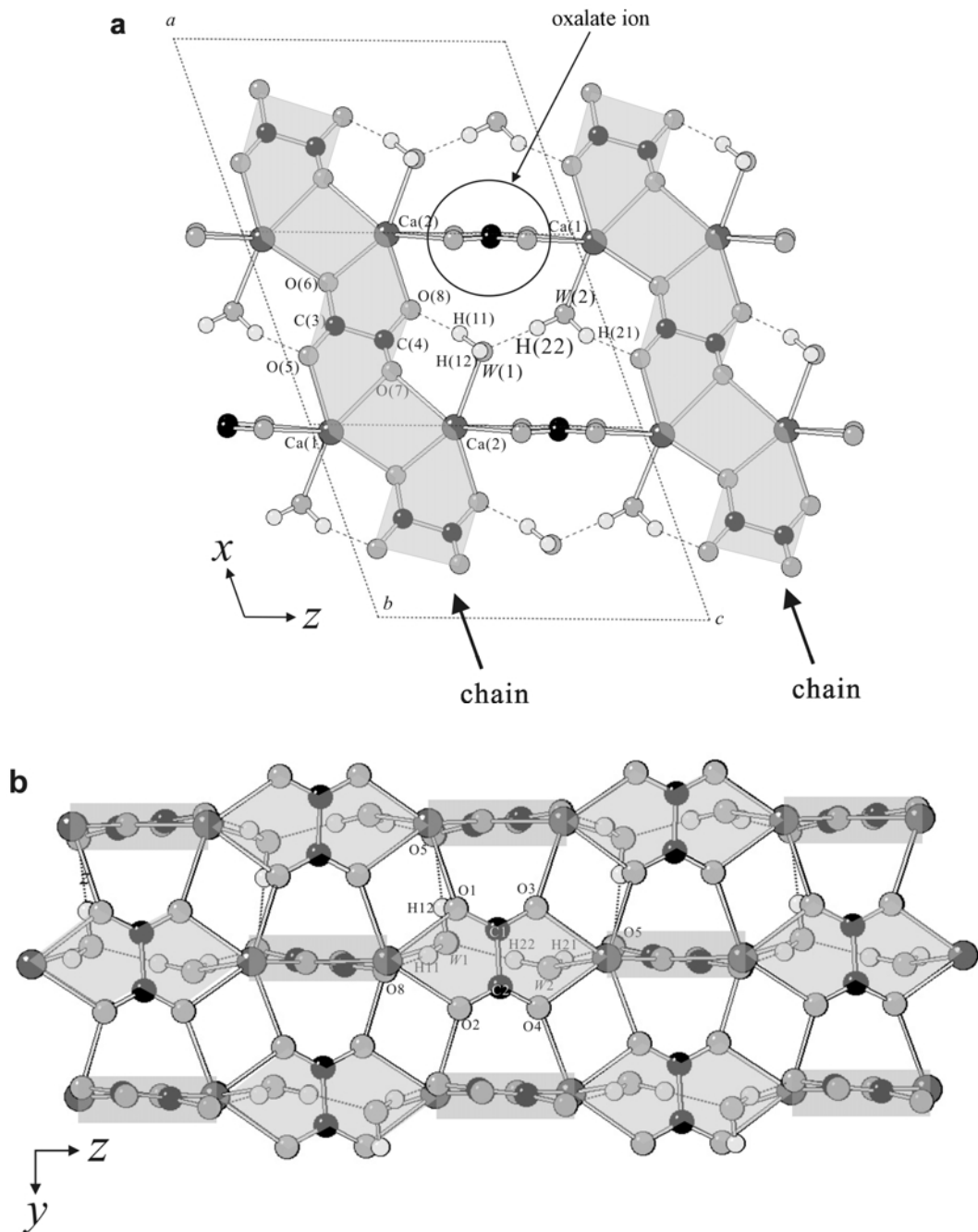


FIG. 3. (a) The structure of whewellite at 123 K, projected down (010). The shaded zigzag chain structure consists of calcium and oxalate ions. These chains are linked by oxalate ions and hydrogen bonds of the intralayered water molecules. The chains form chain-oxalate sheet structures parallel to (010) as a result, and (b) the structure of whewellite at 123 K, projected down (100) shows chain-oxalate sheet structures shaded in the mineral.

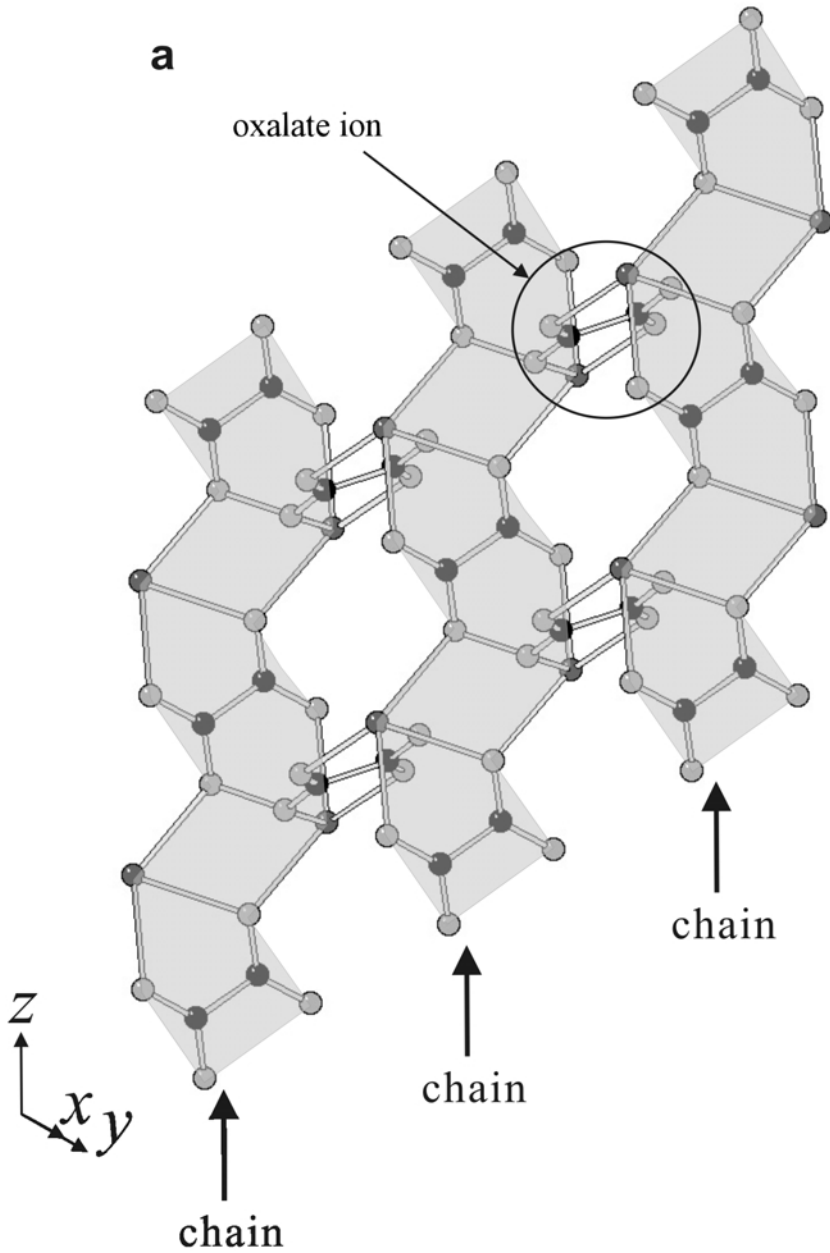


FIG. 4. (*a above*) Crystal structure of caoxite (Deganello *et al.*, 1981). The shaded zigzag chain structure consists of calcium ions and oxalate ions. These chains are linked by oxalate ions to form corrugated sheet structures, and (*b facing page top*) oxalate-chain sheet structures in caoxite. The sheets are corrugated by water molecules intercalated into the sheets with hydrogen bonding.

Domeneghetti, 1980), are shown in Figs 4–5. In caoxite, similar chains in a gradual zigzag are composed of oxalate groups and  $\text{Ca}^{2+}$  ions

running along  $c$  (Fig. 4*a*). These adjacent chains viewed along  $c$ , are bound together by independent oxalate ions to form the structure of wrinkled



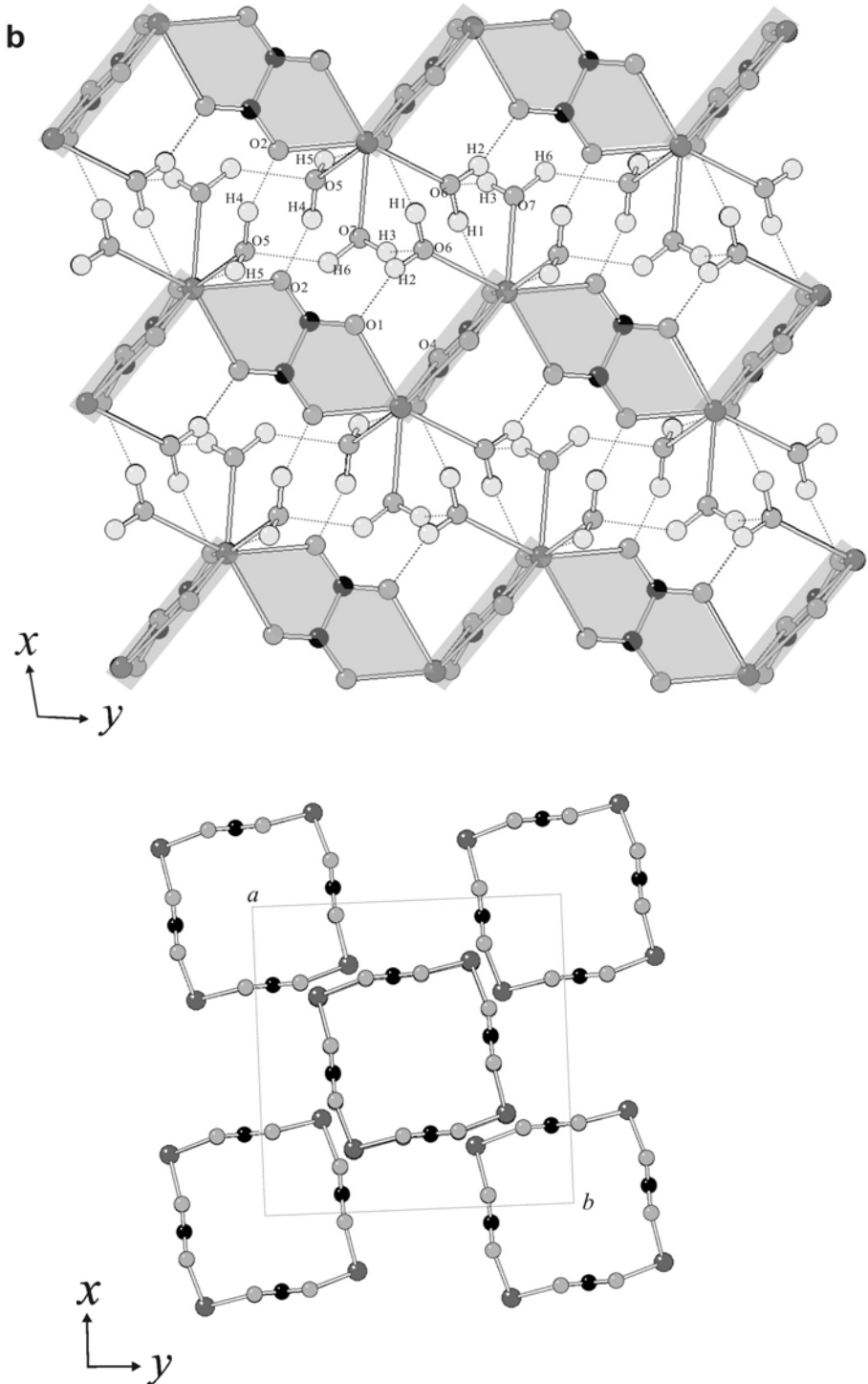


FIG. 5. The channel structure in weddellite consists of calcium ions and oxalate ions, where “zeolitic” water is preserved (Tazzoli and Domeneghetti, 1980).

chain-oxalate sheets (Fig. 4*b*), flattening of which is certainly common in whewellite. In addition, the water molecules in caoxite appear to be intercalated between the sheets to corrugate them by hydrogen bonding (Fig. 4*b*). With increasing temperature and dehydration, i.e. with decreasing hydrogen bonding of the interlayered water molecules, the sheets are flattened and the oxalate ions combining the chains would form bonds with calcium ions included in opposite sheets, giving the whewellite structure as a result (Fig. 3). Additionally, the interlayered-water molecules in caoxite (Fig. 4*b*) turn into the intralayered-water molecules in whewellite that prop up the crystal structure (Fig. 3*b*). The difference between the first dehydration temperature of caoxite (at 85.1°C) and whewellite (at 166.9°C) reveals that the latter rather than the former remains stable in crystal structures against temperature variations. The high dehydration temperature may lead to the more common

occurrence of whewellite than of caoxite in nature. In contrast, such a sheet structure with oxalate chains cannot be found in weddellite (Fig. 5). Alternatively, oxalate groups and  $\text{Ca}^{2+}$  ions in weddellite constitute the channel structure, where "zeolitic" water is preserved (Tazzoli and Domeneghetti, 1980). This channel structure holding water molecules is the most characteristic feature of weddellite; thus the crystal structure of weddellite is appreciably different from those of whewellite and caoxite having the sheet structure.

The IR spectra for three calcium oxalate hydrate minerals are shown in Fig. 6. Throughout a range of IR spectra observed, whewellite and caoxite bear a close similarity, differing from weddellite substantially (Fig. 6). A similarity in the O–C–O antisymmetric stretching vibration around  $1600\text{ cm}^{-1}$  and the O–C–O symmetric stretching vibration around  $1400\text{ cm}^{-1}$  is a parallel between the structures of whewellite and caoxite. This similarity indicates a

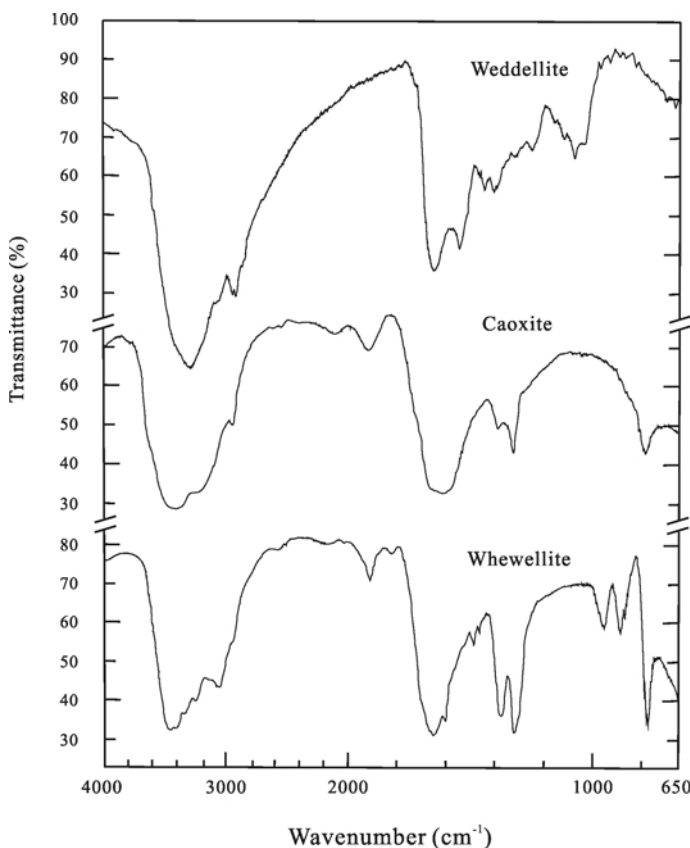


FIG. 6. FTIR spectra of calcium oxalate hydrate minerals.

common feature in the geometry and orientation of the cation ( $\text{Ca}^{2+}$ )–anion  $[(\text{C}_2\text{O}_4)^{2-}]$  bonds between them. It should be noted that the bonding mode of oxalate ion in caoxite might be maintained before and after the dehydration. The O–H-stretching bands of whewellite and caoxite occurred at  $3476\text{ cm}^{-1}$  and  $3429\text{ cm}^{-1}$ , respectively, whereas that of weddellite was located at  $3286\text{ cm}^{-1}$ . It can be inferred that the similarity in the O–H bands is directly related to that in coordinated environments of water molecules between the two crystal structures, though the broader bands in caoxite may suggest a less-ordered molecular arrangement than those in whewellite.

Although the water content of weddellite is closer to that of caoxite than of whewellite, caoxite easily transforms into whewellite as a result of dehydration, without an intermediate weddellite stage. The sheet structures, which consist of oxalate anions and Ca cations, are common to caoxite and whewellite and not resident in weddellite. This structural similarity may provide special facilities for the direct transformation of caoxite into whewellite. In addition, the dehydration of the interlayered water molecules in caoxite could lead to conformation of the intralayered water molecules in whewellite. The observation that the dehydration temperature of the former is lower than that of the latter may provide an explanation for the more common occurrence of the latter in nature. In the present study, the difference in conformation of the water molecules in the crystal structures may also be applicable in terms of the thermal stability of other hydrous minerals common in nature.

### Acknowledgements

Single crystal X-ray data collections were carried out in the Chemical Analysis Centre, University of Tsukuba. We thank two anonymous reviewers for helpful comments and editorial assistant A. Sartbaeva for improving this manuscript.

### References

Arnott, H.J., Pautard, E.G.F. and Steinfink, H. (1965) Structure of calcium oxalate monohydrate. *Nature*, **208**, 1197–1198.  
 Basso, R., Lucchetti, G., Zefiro, L. and Palenzona, A. (1997) Caoxite,  $\text{Ca}(\text{H}_2\text{O})_3(\text{C}_2\text{O}_4)$ , a new mineral from the Cerchiara mine, northern Apennines, Italy.

*Neues Jahrbuch für Mineralogie, Monatshefte*, 84–96  
 Beurskens, P.T., Admiraal, G., Bosman, W.P., de Gelder, P., Israel, R. and Smits, J.M.M. (1999) The DIRDIF-99 program system. *Technical report of the Crystallography Laboratory*, University of Nijmegen, The Netherlands.  
 Cocco, G. (1961) The structure of whewellite. *Atti della Accademia nazionale dei Lincei. Classe di scienze fisiche, matematiche e naturali. Rendiconti. Serie ottava*, **31**, 292–298.  
 Cocco, G. and Sabelli, C. (1962) Structure of whewellite with electronic computer. *Atti della Società Toscana di scienze naturali. Processi verbali*, **69**, 289–298.  
 Deganello, S. and Piro, E.O. (1981) The crystal structure of calcium oxalate monohydrate (whewellite). *Neues Jahrbuch für Mineralogie, Monatshefte*, 81–88.  
 Deganello, S., Kampf, R.A. and Moore, B.P. (1981) The crystal structure of calcium oxalate trihydrate:  $\text{Ca}(\text{H}_2\text{O})_3(\text{C}_2\text{O}_4)$ . *American Mineralogist*, **66**, 859–865.  
 Frost, R.L. and Weier, M.L. (2003) Thermal treatment of weddellite – a Raman and infrared emission spectroscopic study. *Thermochimica Acta*, **406**, 221–232.  
 Frost, R.L. and Weier, M.L. (2004) Thermal treatment of whewellite – a thermal analysis and Raman spectroscopic study. *Thermochimica Acta*, **409**, 79–85.  
 Gaines, R.V., Skinner, H.C.W., Foord, E.E., Mason, B. and Rosenzweig, A. (1997) *Dana's New Mineralogy: the System of Mineralogy of James Dwight Dana and Edward Salisbury Dana*, 8<sup>th</sup> edition. 1011 pp., John Wiley & Sons, New York.  
 Hoffman, W. (1961) On the crystal structure of whewellite,  $\text{Ca}(\text{C}_2\text{O}_4)\cdot\text{H}_2\text{O}$ . *Fortschritte der Mineralogie*, **39**, 346–347.  
 Klopogge, T.J., Boström, E.T. and Weiler, L.M. (2004) In situ observation of the thermal decomposition of weddellite by heating stage environmental scanning electron microscopy. *American Mineralogist*, **89**, 245–248.  
 Leavens, B.P. (1968) New data on whewellite. *American Mineralogist*, **53**, 455–463.  
 Morishige, K., Yoshida, M., Murakami, H., Senoh, N., Kamei, K. and Nishikawa, Y. (1999) Characterization of calcium oxalate hydrate precipitations by the infrared spectrum and X-ray powder diffracton method and its urinary calculi analysis. *Journal of the Faculty of Science and Technology, Kinki University*, **35**, 53–59 (in Japanese with English abstract).  
 Simons, E.L. and Newkirk, A.E. (1964) Calcium oxalate monohydrate guide to the interpretation of thermogravimetric measurement. *Talanta*, **11**, 549–571.  
 Sterling, C. (1965) Crystal-structure analysis of weddel-

- lite,  $\text{CaC}_2\text{O}_4 \cdot (2+x)\text{H}_2\text{O}$ . *Acta Crystallographica*, **18**, 917–921.
- Tazzoli, V. and Domeneghetti, C. (1980) The crystal structures of whewellite and weddellite: re-examination and comparison. *American Mineralogist*, **65**, 327–334.
- Tomažic, B. and Nancollas, G.H. (1979) The kinetics of dissolution of calcium oxalate hydrates. *Journal of Crystal Growth*, **46**, 355–361.
- Watkin, D.J., Prout, C.K., Carruthers, J.R. and Betteridge, P.W. (1996) *CRYSTALS*. Issue 10, Chemical Crystallography Laboratory, Oxford, UK.
- [*Manuscript received 11 May 2004; revised 10 January 2005*]